Experimental Gerontology 223 (2026) 113257

Contents lists available at ScienceDirect

Experimental Gerontology

journal homepage: www.elsevier.com/locate/expgero

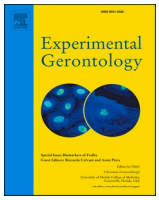

From antioxidant to senotherapeutic: Repurposing n-acetylcysteine to counteract senescence *via* the HuR pathway in human endothelial cells

Lucrezia Irene Maria Campagnoli [a], Nicoletta Marchesi [a], Annalisa Barbieri [a], Nicoletta Galeotti [b], Alessia Pascale [a,*]

[a] Department of Drug Sciences, Section of Pharmacology, University of Pavia, Pavia, Italy
[b] Department of Neuroscience, Psychology, Drug Research and Child Health (NEUROFARBA), Section of Pharmacology and Toxicology, University of Florence, Florence, Italy

ARTICLE INFO

Section Editor: Anna Picca

Keywords:
Cellular senescence
N-acetylcysteine
Drug repurposing
HuR
HUVECs

ABSTRACT

Cellular senescence plays a dual role in physiology and pathology. While it contributes to tumour suppression and tissue repair, its persistence promotes chronic inflammation, tissue dysfunction, and age-related diseases. Oxidative stress is a major driver of this process, and the RNA-binding protein HuR serves as a regulator by stabilizing transcripts encoding antioxidant and stress-response proteins. In this study, we established an *in vitro* model of replicative senescence using human umbilical vein endothelial cells (HUVECs) and investigated the potential anti-aging effects of *N*-acetylcysteine (NAC), an antioxidant and glutathione precursor. Late-passage HUVECs exhibited a senescent phenotype, including enlarged morphology, increased senescence-associated (SA)-β-galactosidase activity, elevated reactive oxygen species (ROS) levels, and upregulation of p16 and p21 proteins. We observed a progressive decline in HuR expression from early to late passages. NAC treatment counteracted these hallmarks, significantly decreasing ROS and p21 levels. Notably, NAC restored HuR expression and its protective targets, MnSOD and HSP70, and reduced inflammatory markers (IL-6 and TNF-α) levels. These findings suggest that the decline of the HuR-protective axis is a critical driver of endothelial senescence and demonstrate that NAC can mitigate aging hallmarks, representing a promising therapeutic strategy to target aging-related dysfunctions.

1. Introduction

Cellular senescence, a process leading to irreversible cell cycle arrest, is triggered by several intrinsic and extrinsic cellular stressors, including DNA damage, oxidative stress (OS), oncogene activation, mitochondrial dysfunction, and telomere shortening. The physiological significance of senescence in organisms remains a subject of debate. While it is considered beneficial due to its proposed role as a potent anti-cancer mechanism and its key functions in embryonic development and wound healing, it is simultaneously deemed detrimental as it limits tissue regeneration, thereby contributing to aging, persistent inflammation, and progression of age-related pathologies, including neurodegenerative disorders. This complex intracellular process is initiated upon the detection of one or more stressful stimuli. Specifically, following cell cycle exit, cells undergo progressive morphological changes, exhibit nuclear remodelling, activate anti-apoptotic pathways, and secrete a wide array of factors, including cytokines, chemokines, growth factors, proteases, small extracellular vesicles, bioactive lipids, collectively known as the "senescence-associated secretory phenotype" (SASP) (Herranz and Gil, 2018). Moreover, these cells exhibit mitochondrial and lysosomal dysfunction, evidenced by increased levels of reactive oxygen species (ROS) and senescence-associated (SA)-β-galactosidase activity (Herranz and Gil, 2018). As mentioned, a key contributor to senescence is increased OS, a condition resulting from an imbalance between pro-oxidant stimuli and antioxidant defences. Key signaling pathways that trigger senescence rely on the deregulation of ROS/RNS (reactive nitrogen species), primarily by impairing the antioxidant system. This damage is commonly associated with the dysfunction of the transcription factor Nrf2 (nuclear factor erythroid 2-related factor 2) and the activation of redox-sensitive signaling pathways, such as those controlled by nuclear factor kappa-light-chain-enhancer of activated B cells (NF-kB) (Varesi et al., 2022). Specifically, under OS, Nrf2

* Corresponding author.
E-mail addresses: lucreziairenemaria.campagnoli@unipv.it (L.I.M. Campagnoli), nicoletta.marchesi@unipv.it (N. Marchesi), annalisa.barbieri@unipv.it (A. Barbieri), nicoletta.galeotti@unifi.it (N. Galeotti), alessia.pascale@unipv.it (A. Pascale).

https://doi.org/10.1016/j.exger.2026.113257
Received 29 April 2026; Received in revised form 10 July 2026; Accepted 28 July 2026
Available online 31 July 2026

dissociates from its inhibitor Keap1, translocates to the nucleus, and binds to the antioxidant response element (ARE) to induce the expression of several protective enzymes, including manganese-dependent superoxide dismutase (MnSOD), which detoxifies the cell from ROS (Mallucci et al., 2022; Ngo and Duennwald, 2022). Additionally, the defensive role of the heat shock proteins 70 (HSP70) family has been well-recognized in the context of OS. This highly conserved family comprises intracellular proteins that prevent protein misfolding and aggregation through their chaperone activity, thereby protecting cells from apoptosis (Campagnoli et al., 2024). Another major driving force in senescence is the activation of molecular cascades associated with p53/p21 and p16 (Varesi et al., 2022). Both p16 and p21 are cyclin-dependent kinase inhibitors that induce cell cycle arrest. Specifically, p16 prevents the phosphorylation of retinoblastoma (Rb) protein contributing to G1/S cell cycle arrest (Rayess et al., 2012), while p21, activated by the transcription factor p53 (involved in the regulation of cell division, prevention of uncontrolled proliferation, and suppression of tumorigenesis), mediates G1/S and G2/M arrest by modulating the activity of specific p53 targets (Al Bitar and Gali-Muhtasib, 2019). Several studies suggest that post-transcriptional regulatory mechanisms play a key role during cellular senescence (Varesi et al., 2023). In this regard, the ubiquitous RNA-binding protein HuR (a member of the ELAV family), following intra- and extracellular inputs, acts as a central regulator of many cellular functions, including survival, proliferation, and apoptosis, as well as OS and inflammatory processes. Furthermore, HuR has been identified as a critical player in the senescence process: its depletion accelerates the senescent phenotype by reducing the expression of proliferative genes, while its overexpression delays replicative senescence (Lee et al., 2018). Of particular interest to this study, HuR protein, *via* its RNA recognition motifs (RRMs), specifically binds several mRNA targets, including MnSOD and HSP70 transcripts, by modulating their stability and promoting the expression of their relative protective proteins (Amadio et al., 2008; Mallucci et al., 2022).

Considering its detrimental impact on a wide range of chronic and age-related conditions, cellular senescence has emerged as a compelling target for personalized therapies. Indeed, accumulating evidence supports a causative role for senescent cells in the pathogenesis of various metabolic, cardiovascular, renal, hepatic, musculoskeletal, and neurodegenerative disorders (Kaur and Farr, 2020). Preclinical studies demonstrate that the reduction of senescent cells (achieved either genetically or pharmacologically) can mitigate or even reverse features of frailty, metabolic dysfunction, organ fibrosis, and vascular or neurodegenerative pathologies, thereby improving both lifespan and healthspan in animal models (Amaya-Montoya et al., 2020). This systematic approach, by addressing fundamental aging mechanisms rather than individual diseases, offers the possibility of simultaneously preventing or treating multiple comorbidities with a single intervention (Khosla et al., 2020). Consequently, targeting cellular senescence is widely regarded as a promising strategy to delay or ameliorate a broad spectrum of age-related diseases, with significant potential for translational impact on human health. In this regard, current anti-senescence strategies include the use of senomorphic agents. Unlike senolytics, these compounds do not trigger apoptosis; instead, they attenuate the harmful secretome of senescent cells and reduce the overall senescent burden by modulating specific molecular pathways (Cong et al., 2025). *N*-acetylcysteine (NAC), a well-known mucolytic agent with potent antioxidant properties, may represent a prominent candidate for drug repurposing in this context. As a direct precursor to glutathione (GSH; an endogenous antioxidant that protects cells from damage by neutralizing harmful ROS), NAC is essential for maintaining cellular health. Due to its established safety profile and its ability to restore intracellular GSH, NAC is clinically administered for various metabolic, respiratory, and neurotoxic conditions (Elbini Dhouib et al., 2016). Given that endothelial cell senescence is considered a primary contributor to human aging, thus playing a relevant role in the onset of age-related disorders (Bloom et al., 2023), in this study, according to Yi et al. (Yi et al., 2020), we employed human umbilical vein endothelial cells (HUVECs) as a model of replicative senescence, as they naturally undergo senescence without exogenous stimuli (Grosse et al., 2020). Specifically, we first set up an *in vitro* model of senescence by assessing morphological changes and key markers, including the cell cycle inhibitors p16 and p21, SA-β-galactosidase activity, and ROS accumulation. Subsequently, we investigated the potential anti-aging properties of NAC, evaluating its effects on the aforementioned markers, as well as on specific pro-inflammatory cytokines [interleukin 6 (IL-6) and tumour necrosis factor α (TNF-α)], and on the protective HuR/MnSOD and HSP70 pathways.

2. Materials and methods

2.1. Cell culture and treatment

HUVECs were obtained from Sigma, plated in 25 cm^2 flasks, and cultured in an all-in-one ready-to-use medium (Endothelial Cell Growth Medium; Sigma-Aldrich, St. Louis, MO, USA). The flasks were incubated at 37 °C in a humidified atmosphere containing 5% CO_2. Cells were treated with NAC (Sigma-Aldrich, St. Louis, MO, USA) at 1 mM for 24 and 48 h.

2.2. Morphology

Cell morphology was observed by using Alexa Fluor® 555 Phalloidin (Cell Signaling Technology, Denver, CO, USA). In detail, a cell suspension of 2.5×10^4 cells in 200 μL was seeded on slides placed in a 24-well plate. After treatment, cells were washed with PBS, fixed for 20 min at room temperature (RT) using 4% formaldehyde, and re-washed three times with PBS for 5 min each. Once fixed, cells were permeabilized with Triton X-100 0.1%, washed once with PBS, and incubated with Alexa Fluor 555 Phalloidin (1:75) for 15 min at RT in the dark. After incubation, cells were washed once with PBS for 15 min, incubated with HOECHST 3342 (1:10000) (Abcam, Cambridge, UK) for 10 min at RT, and then the slides were mounted on the cover slides. The images were acquired with confocal and wide-field microscopes.

2.3. Cell viability assay

Mitochondrial enzymatic activity was estimated using the MTT [3-(4,5-dimethylthiazol-2-yl)-2,5-diphenyltetrazolium bromide] assay (Sigma-Aldrich, St. Louis, MO, USA) according to a previously published protocol (Fahmideh et al., 2022). Briefly, a cell suspension of 2.5×10^4 cells/well in 200 μL was seeded into 96-well plates. Following the treatment, 50 μL of MTT was added to each well. After incubation at 37 °C for 3 h, the formed purple formazan crystals were solubilized in 100 μL of dimethyl sulfoxide (DMSO) (Sigma-Aldrich, St. Louis, MO, USA) for 10 min under agitation. The absorbance values were measured at 595 nm using a Synergy HT microplate reader (BioTek Instruments, Vermont, USA), and the results were expressed as % with respect to the control.

2.4. ROS levels

The production of ROS was investigated by using the ROS-Glo™ H_2O_2 Assay Protocol (Promega, Madison, WI, USA) following the manufacturer's instructions. Briefly, a cell suspension of 2×10^4 cells/well in 200 μL was seeded into 96-well opaque plates. Four hours after the end of treatment, 20 μL of H_2O_2 substrate solution was added to each well, and the 96-well plate was incubated at 37 °C, 5% CO_2 for 4 h. After incubation, ROS-Glo™ Detection Solution was added to each well, the 96-well plate was incubated at RT for 20 min, and the luminescence was measured by using an INNO-S microplate reader (Aurogene, Rome, IT).

2.5. SA-β-galactosidase activity

The SA-β-galactosidase activity was tested by using the Mammalian SA-β-Galactosidase Assay Kit (ThermoFisher, Waltham, MA, USA) following the manufacturer's instructions. Briefly, a cell suspension of 2 × 10^4 cells/well in 200 μL was seeded into 96-well plates. Following the treatment, cells were washed once with Dulbecco's phosphate buffer saline (PBS) (Euroclone, Milan, IT), and 100 μL of SA-β-Galactosidase Assay Reagent was added to each well. After incubation at 37 °C for 30 min, the absorbance values were measured at 405 nm using a Synergy HT microplate reader (BioTek Instruments, Vermont, USA).

2.6. ELISA

The IL-6 expression in the medium was investigated by using the Human IL-6 ELISA Kit (Ray Biotech, Norcross, GA, USA). The Ray-Bio® Human IL-6 ELISA kit is an *in vitro* enzyme-linked immunosorbent assay for the quantitative measurement of human IL-6 in culture supernatants. This assay employs an antibody specific for human IL-6 coated on a 96-well plate. Standards and samples are added into the wells, and IL-6 present in each sample is bound to the wells by the immobilized antibody. After washing the wells, a biotinylated anti-human IL-6 antibody is added. Unbound biotinylated antibody is removed by further washing, followed by the addition of Horseradish peroxidase (HRP)-conjugated streptavidin. After a final wash, a TMB (3,3,5,5′-tetramethylbenzidine) substrate solution is added to the wells, developing a colour proportional to the amount of bound IL-6. The reaction is then halted with a stop solution, changing the colour from blue to yellow, and the absorbance is measured at 450 nm using a Synergy HT microplate reader (BioTek Instruments, Vermont, USA).

2.7. Western blotting

The Western blotting procedure was performed according to the protocol previously described by our group (Campagnoli et al., 2024). The protein content of each sample was determined according to Bradford's method, using bovine serum albumin (BSA; Sigma-Aldrich, St. Louis, MO, USA) as a standard. Proteins were diluted in Sodium Dodecyl Sulphate (SDS) protein gel loading solution 2×, boiled for 5 min at 95 °C, and separated onto 12% SDS polyacrylamide gel electrophoresis (PAGE). After running, proteins were transferred to nitrocellulose membranes (porosity: 0.2 μm) for 2 h at a constant electrical current of 250 mA. As a molecular weight marker, a standard mixture with coloured proteins and a known molecular weight (Amersham, Chicago, CA, USA) was used. Unspecific sites were blocked with 5% BSA in TBST buffer [10 mM of Tris-HCl, 100 mM of NaCl, 0.1% (v/v) Tween 20, pH 7.5] at RT for 1 h, and then the membranes were incubated with the primary antibodies overnight at 4 °C under gentle agitation. The anti-p16, the anti-p21, the anti-TNF-α, and the anti-MnSOD (all Cell Signaling Technology, Denver, CO, USA) monoclonal antibodies were diluted 1:500 in TBST buffer containing 5% (v/v) BSA, based on each data sheet. The anti-HuR and the anti-HSP70 (all Santa Cruz Biotech, Dallas, TX, USA) monoclonal antibodies were diluted 1:1000 in TBST buffer containing 5% (v/v) BSA. The next day, the membranes were washed and then incubated for 1 h with the secondary antibodies diluted according to the relative data sheet. The membrane signals were detected by chemiluminescence, employing an Imager Amersham 680 detection system and using ponceau (30–95 kDa) (Biotium, Fremont, CA, USA) to normalize the data. The densitometric analysis of the Western blots was performed using the ImageJ 1.54 image-processing program, after image acquisition.

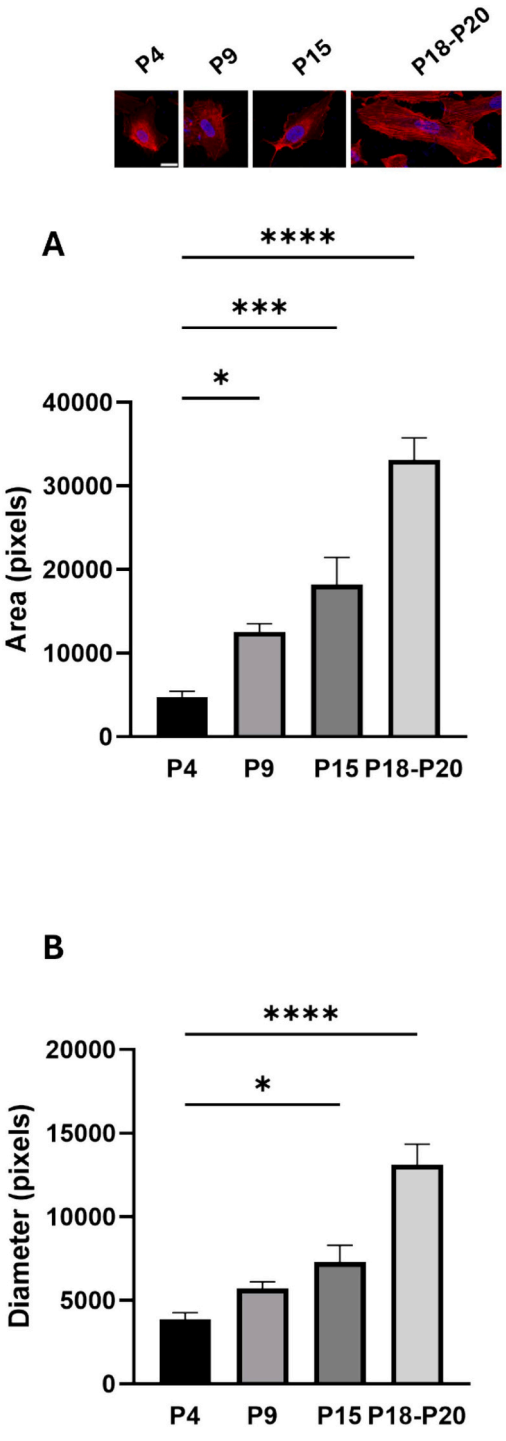

Fig. 1. Morphological characterization of HUVECs during replicative senescence. Upper side: cropped representative images of the cytoskeleton (red; Alexa Fluor 555 Phalloidin) of HUVECs obtained with a confocal microscope (scale bar = 20 μm); lower side: analysis of the area (A) and the diameter (B) of HUVECs from P4 to P18-P20. The results are expressed as mean ± S.E.M.; data were analysed by one-way ANOVA followed by Tukey's multiple comparisons test, $n = 15$ independent samples; *$p < 0.05$, ***$p < 0.001$, ****$p < 0.0001$ *vs* P4. P4 = HUVECs at passage 4; P9 = HUVECs at passage 9; P15 = HUVECs at passage 15; P18-P20 = HUVECs between passage 18 and 20. (For interpretation of the references to colour in this figure legend, the reader is referred to the web version of this article.)

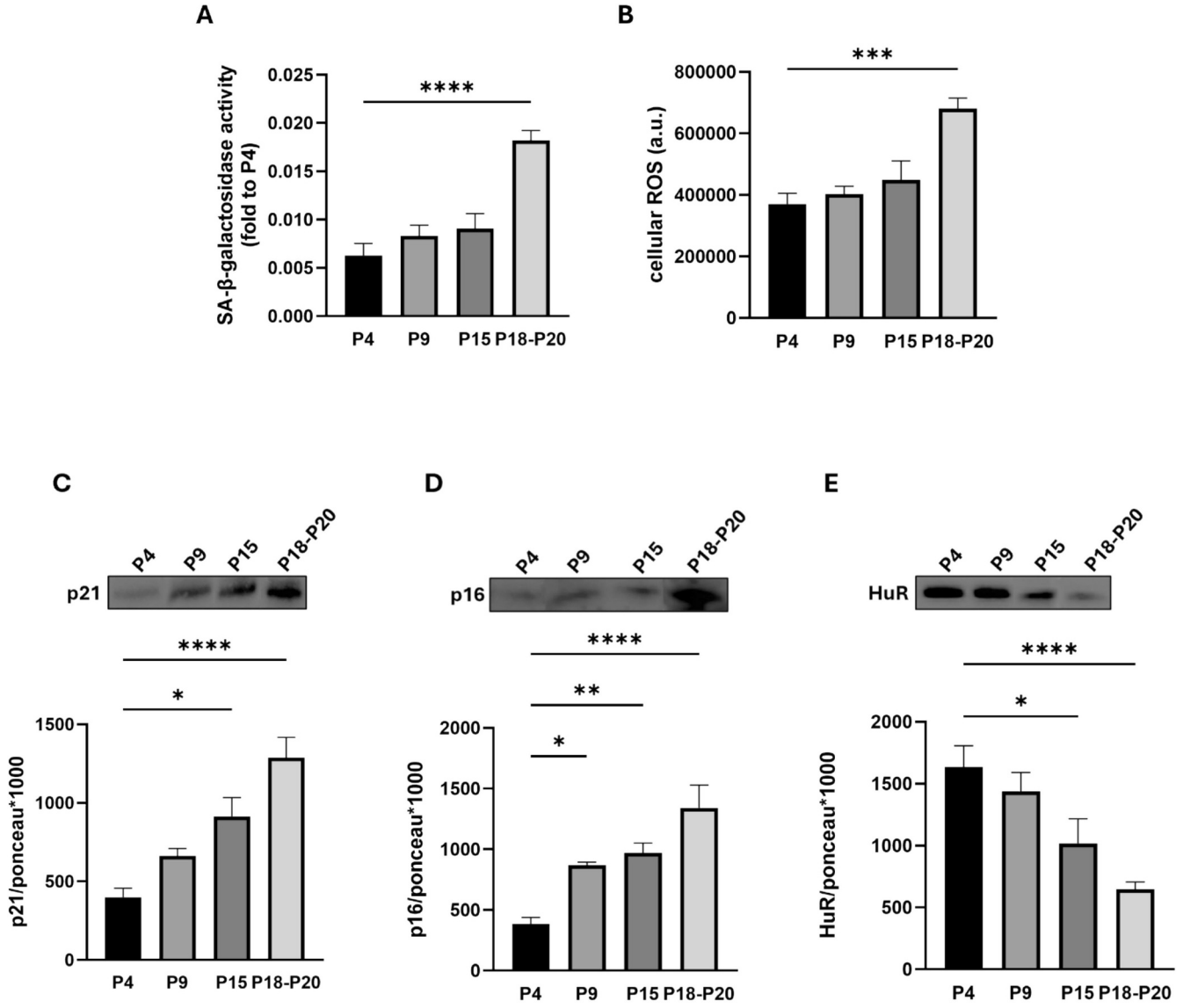

Fig. 2. Changes in senescence-associated parameters and HuR levels during HUVECs replicative aging. A) SA-β-galactosidase activity and B) cellular ROS levels in HUVECs from early to late-passages. The results are expressed as mean ± S.E.M.; ***$p < 0.001$, ****$p < 0.0001$ *vs* P4; statistical analysis was performed using the one-way ANOVA followed by Tukey's multiple comparisons test, $n = 15$ independent samples for SA-β-galactosidase activity, $n = 5$–8 for cellular ROS levels. P21 (C), p16 (D), and HuR (E) protein expression in HUVECs from early to late passages. Upper side: cropped representative Western blotting images. Lower side: densitometric analysis. The results are expressed as the mean grey level ratios × 10^3 (mean ± S.E.M.) for p21, p16, and HuR immunoreactivities, measured by Western blotting and normalized to ponceau signals. Data were analysed by the one-way ANOVA followed by Tukey's multiple comparisons test, $n = 5$–10 independent samples; *$p < 0.05$, **$p < 0.01$, ****$p < 0.0001$ *vs* P4. P4 = HUVECs at passage 4; P9 = HUVECs at passage 9; P15 = HUVECs at passage 15; P18-P20 = HUVECs between passage 18 and 20.

2.8. Real-time quantitative RT-PCR

RNA was extracted from total homogenates using RNeasy Micro Plus Kit (Qiagen, Hilden, Germany). The reverse transcription was performed following standard procedures. PCR amplifications were carried out using the Rotor-Gene Q (Qiagen, Hilden, Germany) in the presence of QuantiTect SYBR Green PCR mix (Qiagen, Hilden, Germany) with primers predesigned by SIGMA. Primer sequences used were as follows: forward: 5-GATCAGACTACAGGTTTGTC-3 and reverse: 5-TTGAAA CTGGTAATTGCCTC-3 (for HuR); forward: 5-TCGTCCTCCGCTTTG TACTT-3 and reverse: 5- AGGCCAACAAGATCACCATC-3 (for HSP70); forward: 5-CGATCGTTATGCTGAGTATG-3 and reverse: 5-TCAAT-CACTTGCCCAATAAC-3 (for MnSOD); forward: 5-CAGCAAGAGCACAA-GAGGA-3 and reverse: 5-CAACTGTGAGGAGGGGAGATT-3 (for GAPDH). The GAPDH mRNA was chosen as control since it is relatively stable during all the treatments, and it is unaffected by HuR because it does not possess ARE sequences (not shown). HuR, HSP70 and MnSOD mRNA expression was normalized over GAPDH mRNA.

2.9. Statistical analysis

The GraphPad Prism statistical package (version 10, San Diego, CA, USA) was used for the statistical analysis. The data were analysed by analysis of variance (ANOVA), followed, when significant, by an appropriate *post hoc* comparison test, as detailed in the legends. A *p*-value below 0.05 was considered statistically significant. The results are expressed as the mean grey level ratios x 10^3 (mean ± S.E.M.) of the protein immunoreactivities measured by Western blotting and normalized on ponceau signals. The N in the legend figure indicates the number of independent experiments, each with 2–3 replicates.

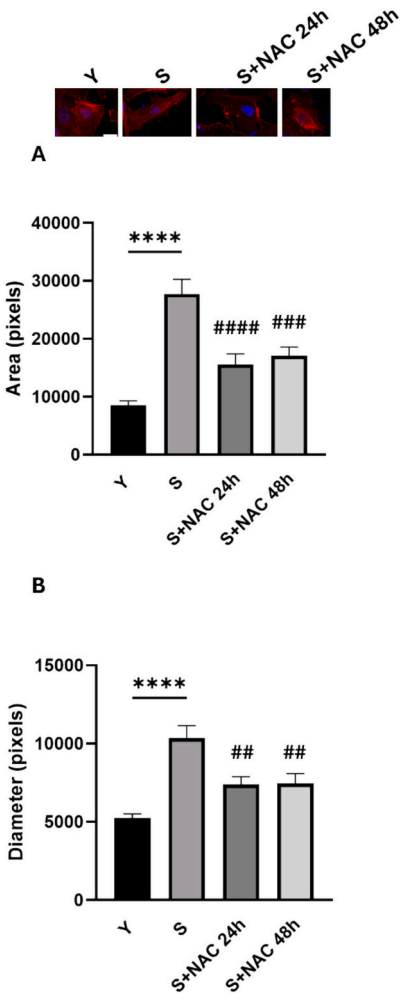

Fig. 3. Effect of *N*-acetylcysteine on the morphology of senescent HUVECs. Upper side: cropped representative images of the cytoskeleton (red; Alexa Fluor 555 Phalloidin) of HUVECs obtained with a widefield microscope (scale bar = 10 μm); lower side: quantitative analysis of the area (A) and the diameter (B) of young (Y), senescent (S), and S HUVECs after 24 and 48 h of *N*-acetylcysteine (NAC) treatment. The results are expressed as mean ± S.E.M.; data were analysed by one-way ANOVA followed by Tukey's multiple comparisons test, $n = 15$ independent samples; $^{****}p < 0.0001$ (Y *vs* S); $^{\#\#}p < 0.01$, $^{\#\#\#}p < 0.001$, $^{\#\#\#\#}p < 0.0001$ (S *vs* S + NAC). S + NAC 24 h = S cells after 24 h of NAC treatment; S + NAC 48 h = S cells after 48 h of NAC treatment. (For interpretation of the references to colour in this figure legend, the reader is referred to the web version of this article.)

3. Results

3.1. Characterization of an in vitro model of replicative senescence

In the first part of the study, we established an *in vitro* model of replicative senescence by examining morphology, key senescence-associated markers (SA-β-galactosidase activity, ROS levels, p21, and p16), and HuR protein expression in HUVECs from early (P4) to late passages (P18-P20). As shown in Fig. 1, cellular morphology underwent significant changes during replicative aging; the small, highly organized morphology characteristic of P4 cells progressively transitioned toward an enlarged and pleomorphic phenotype. This shift was quantitatively confirmed by an increase in cell area (Fig. 1A) and diameter (Fig. 1B) in late-passage cells compared to their younger counterparts.

Subsequently, we studied senescence-associated metabolic (SA-β-galactosidase activity and ROS levels) and molecular (p21 and p16) parameters, together with HuR protein content. The results reported in Fig. 2 suggest clear differences in these parameters between HUVECs at P4 and P18-P20. Regarding the metabolic parameters, we observed a progressive increase in SA-β-galactosidase activity (Fig. 2A) and intracellular ROS levels (Fig. 2B) from early to late-passage HUVECs, with a significant increase in the older ones. Consistent with this senescent phenotype, Western blotting analysis demonstrated a significant up-regulation of the cell cycle inhibitors p21 and p16. Specifically, a substantial increase in p21 (Fig. 2C) and p16 (Fig. 2D) protein content was observed from P4 to P18-P20. In contrast, HuR protein expression followed an opposite trend (Fig. 2E); indeed, a significant and progressive decrease in HuR levels was detected from younger to older cells, with the lowest expression observed in the P18-P20 group.

Taken together, these findings indicate that, in our model of "physiological aging", HUVECs transition between passages 18 and 20 into a definitive senescent state. For clarity, hereafter, early-passage (P4-P6) cells will be referred to as 'Y' (Young), while late-passage (P18-P19) senescent cells will be referred to as 'S' (Senescent).

3.2. Investigation of the potential anti-aging effects of NAC

In the second phase of the study, we investigated the potential anti-aging effects of NAC by treating senescent (S) HUVECs with this compound at 1 mM for 24 and 48 h. Notably, in the examined conditions, we neither observed any change in cell viability between young and old cells, nor NAC induced any further modification (Suppl. 1). Then, we evaluated whether NAC treatment could promote a morphological reversion of S cells toward a phenotype more characteristic of young (Y) cells. As illustrated in Fig. 3, exposure to NAC for both 24 and 48 h resulted in a visible reduction in cell size and a more organized cellular architecture. Quantitative analysis showed a significant decrease in both cell area (Fig. 3A) and diameter (Fig. 3B), indicating a shift toward the morphological profile of Y cells.

Subsequently, we evaluated the potential of NAC to modulate senescence-associated metabolic and molecular markers, as well as HuR protein expression, as reported in Fig. 4. Regarding metabolic parameters, the obtained results indicate that NAC induces a decrease in both SA-β-galactosidase activity (Fig. 4A) and intracellular ROS levels (Fig. 4B) in S cells following 24 and 48 h of treatment. Notably, while ROS levels were significantly reduced to values comparable to Y cells within 24 and 48 h, the reduction in SA-β-galactosidase activity appeared less pronounced. To ascertain whether a prolonged exposure could achieve a full reversal, experiments were extended to 72 h; however, the reduction trend remained consistent with that observed at 48 h (data not shown). Consistently, Western blotting analysis revealed a reduction in the protein content of both the molecular markers p21 and p16 (Fig. 4C–D) in S cells upon 24 and 48 h of NAC exposure. In detail, the expression of p21 significantly decreased after 24 h, with a further reduction at 48 h that reached levels similar to those detected in Y cells. Instead, p16 showed a downward trend that did not reach statistical significance. Interestingly, NAC treatment also exerted a significant effect on HuR expression (Fig. 4E); indeed, S cells exhibited a progressive increase in HuR protein content, which became statistically significant after 48 h, effectively restoring the levels observed in Y cells.

Since NAC is able to upregulate the expression of HuR in S cells (Fig. 4E), we investigated its effects on two specific HuR-protective targets: MnSOD and HSP70. Consistent with the trend observed for HuR, NAC treatment is also able to modulate the expression of these proteins, as reported in Fig. 5. Specifically, MnSOD (Fig. 5A) levels were lower in S cells compared to Y ones; these levels were partially restored after 24 h and increased significantly after 48 h of treatment, nearly reaching the levels detected in Y cells. Instead, for HSP70 (Fig. 5B), the low expression in S cells increased significantly already after 24 h of treatment, matching the levels observed in Y cells and persisting through 48 h (Fig. 5B).

To elucidate whether these modifications were also driven by transcriptional regulation, we evaluated the impact of NAC on the mRNA

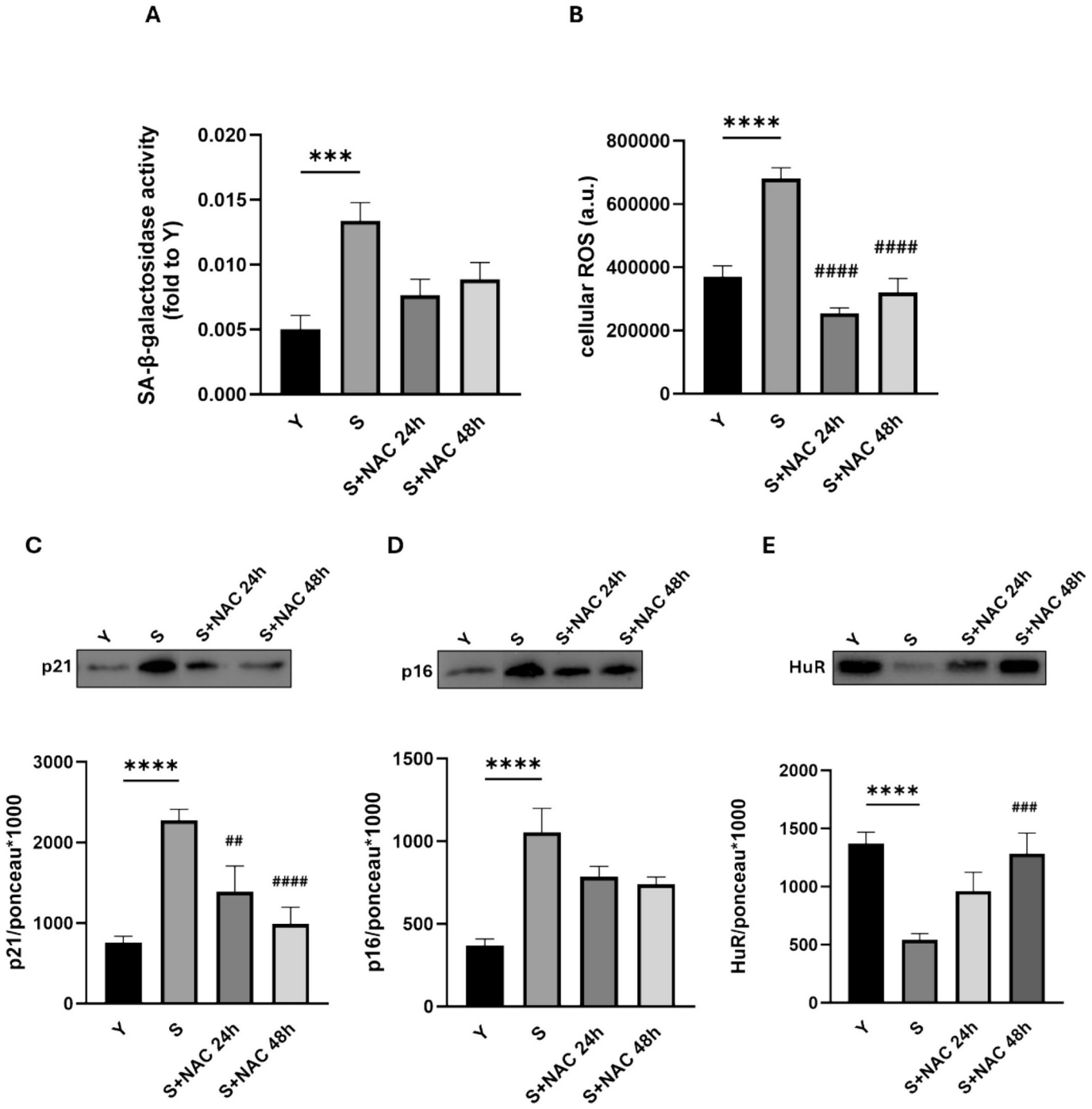

Fig. 4. Effect of *N*-acetylcysteine on senescence-associated markers and HuR expression in senescent HUVECs. A) SA-β-galactosidase activity and B) cellular ROS levels in young (Y), senescent (S), and S HUVECs after 24 and 48 h of *N*-acetylcysteine (NAC) treatment. The results are expressed as mean ± S.E.M.; $^{***}p < 0.001$, $^{****}p < 0.0001$ (Y *vs* S); $^{\#\#\#\#}p < 0.0001$ (S *vs* S + NAC); statistical analysis was performed using the one-way ANOVA followed by Tukey's multiple comparisons test, $n = 6$–8 independent samples for SA-β-galactosidase activity, $n = 5$–6 for cellular ROS levels. P21 (C), p16 (D), and HuR (E) protein expression in Y, S, and S HUVECs after 24 and 48 h of NAC treatment. Upper side: cropped representative Western blotting images; lower side: densitometric analysis. The results are expressed as the mean grey level ratios × 10^3 (mean ± S.E.M.) for p21, p16, and HuR immunoreactivities, measured by Western blotting and normalized to ponceau signals. Data were analysed by the one-way ANOVA followed by Tukey's multiple comparisons test, $n = 5$–10 independent samples; $^{****}p < 0.0001$ (Y *vs* S); $^{\#\#}p < 0.01$, $^{\#\#\#}p < 0.001$, $^{\#\#\#\#}p < 0.0001$ (S *vs* S + NAC). S + NAC 24 h = S cells after 24 h of NAC treatment; S + NAC 48 h = S cells after 48 h of NAC treatment.

levels of HuR and its downstream targets. While no significant variations were detected at 24 h, a remarkable upregulation was observed at 48 h of treatment. Specifically, real-time PCR analysis revealed a significant increase in HuR mRNA levels (S:100% *vs* S + NAC: 211%; * $p < 0.05$, Dunnett's test). Parallel to this, a substantial elevation was found for both MnSOD (S:100% *vs* S + NAC: 321%; * $p < 0.05$, Dunnett's test) and HSP70 (S:100% *vs* S + NAC: 259%; $p < 0.05$, Dunnett's test) transcripts. This transcriptional activation strictly mirrors the upregulation observed at the protein level, confirming that the recovery of the HuR-protective axis by NAC involves, at least in part, a modulation of gene expression.

Lastly, to evaluate the anti-inflammatory potential of NAC in the

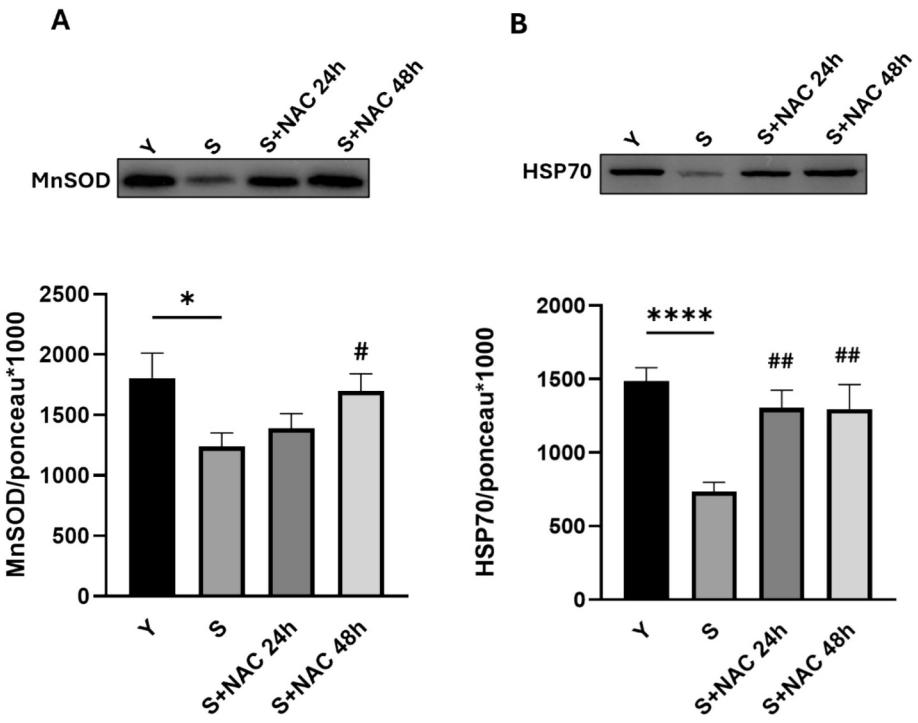

Fig. 5. Protective effect of *N*-acetylcysteine on the expression of MnSOD and HSP70 in senescent HUVECs. Upper side: cropped representative Western blotting images; lower side: densitometric analysis of MnSOD (A) and HSP70 (B) protein expression in young (Y), senescent (S), and S HUVECs after 24 and 48 h of *N*-acetylcysteine (NAC) treatment. The results are expressed as the mean grey level ratios $\times 10^3$ (mean ± S.E.M.) for MnSOD and HSP70 immunoreactivities, measured by Western blotting and normalized to ponceau signals. Data were analysed by the one-way ANOVA followed by Tukey's multiple comparisons test, $n = 6$–9 independent samples; $^{*}p < 0.05$, $^{****}p < 0.0001$ (Y *vs* S); $^{\#}p < 0.05$, $^{\#\#}p < 0.01$ (S *vs* S + NAC). S + NAC 24 h = S cells after 24 h of NAC treatment; S + NAC 48 h = S cells after 48 h of NAC treatment.

context of SASP, we investigated its effects on TNF-α (intracellular) and IL-6 (released in the medium). Our results demonstrate that NAC significantly modulates both cytokines (Fig. 6). In detail, we observed a marked increase in TNF-α (Fig. 6A) expression in S cells compared to Y cells; these high levels were significantly reduced by NAC after 48 h of treatment, restoring the protein content to levels comparable to Y cells. Consistent with the TNF-α profile, we found high extracellular levels of IL-6 (Fig. 6B) in S cells compared to Y cells, and this rise was effectively counteracted as early as 24 h of NAC exposure.

4. Discussion

Aging is a systemic process driven by complex biological mechanisms, among which cellular senescence stands out as a fundamental hallmark (McHugh and Gil, 2018). While transient senescence plays a physiological role in tissue remodelling and wound healing, the chronic accumulation of senescent cells promotes tissue dysfunction and persistent inflammation, fuelling the progression of age-related pathologies (Herranz and Gil, 2018). A central driver in both the initiation and maintenance of the senescent state is OS (Varesi et al., 2022). The excessive accumulation of ROS perturbs redox homeostasis and causes widespread macromolecular damage, particularly to DNA and mitochondria, thereby triggering stress-responsive signaling pathways that drive cell-cycle arrest and senescence (Jomova et al., 2023). One of the earliest and most pivotal outcomes of OS is the activation of the DNA damage response (Coluzzi et al., 2019), which stabilizes p53 and induces the expression of cyclin-dependent kinase inhibitors, such as p21 and p16, ultimately leading to permanent cell-cycle arrest (Mijit et al., 2020). Despite exhibiting altered morphology (increased cell size and flattened shape) and specific gene expression patterns, as well as a loss of replicative capacity, senescent cells remain metabolically active and resistant to apoptosis. A defining feature of this state is the SASP, a complex secretome comprising, as previously mentioned, a broad range of pro-inflammatory cytokines, chemokines, growth factors, proteases, small extracellular vesicles, and bioactive lipids (leukotrienes) that contribute to inflammatory responses and influence both physiological and pathological aging processes (Herranz and Gil, 2018). Moreover, if the senescence state persists, the cells can transition into a "late senescence" phase, characterized by chronic inflammation and a further diversification of the senescent phenotype, which exacerbates local and systemic aging (Herranz and Gil, 2018). Given that endothelial cell senescence is increasingly recognized as a primary trigger for vascular aging, which in turn is implicated in the development of age-related diseases (Bloom et al., 2023), understanding the underlying mechanisms is crucial for developing targeted therapeutic interventions.

In this study, the progressive passaging of HUVECs (up to P18-P20) successfully established a robust *in vitro* model of "natural" aging. The observed morphological shift, from small, organized cells to an enlarged and flattened phenotype, aligns perfectly with structural hallmarks of endothelial aging previously reported in literature (Yi et al., 2020). These morphological changes reflect profound cytoskeletal remodelling that accompanies the loss of proliferative capacity, underscoring a functional decline. While cell viability remained stable (Suppl. 1), indicating that the cells are not dying but rather "arrested", their metabolic profile underwent a dramatic transition. The pronounced increase in SA-β-galactosidase activity and intracellular ROS levels in late-passage cells confirms that lysosomal dysfunction and mitochondrial oxidative stress are core features of our model (Gorgoulis et al., 2019; Hernandez-Segura et al., 2018). Interestingly, recent findings suggest that SA-β-galactosidase activity correlates with enhanced lysosomal biogenesis and metabolic dysfunction in senescent fibroblasts, reinforcing its role as a key senescence biomarker (Franco et al., 2025). Consistent with these data, we observed a significant upregulation of the cyclin-dependent kinase inhibitors p21 and p16 in old HUVECs (Childs

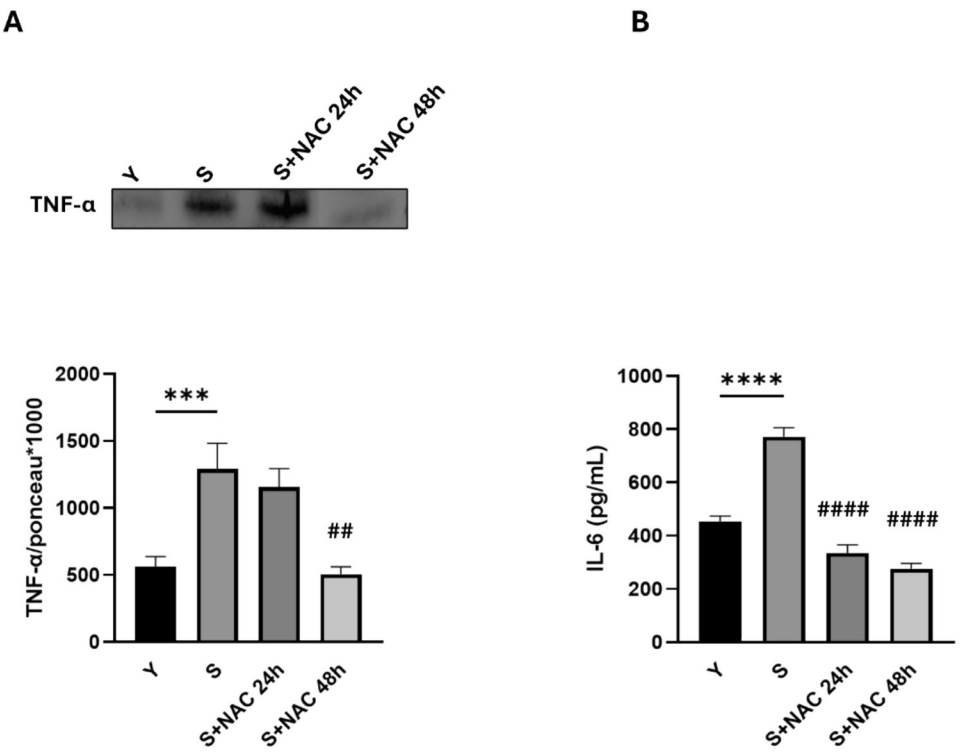

Fig. 6. Anti-inflammatory effect of *N*-acetylcysteine on selected SASP factors in senescent HUVECs. A) Upper side: cropped representative Western blotting images; lower side: densitometric analysis of TNF-α protein expression in young (Y), senescent (S), and S HUVECs after 24 and 48 h of *N*-acetylcysteine (NAC) treatment. The results are expressed as the mean grey level ratios × 10^3 (mean ± S.E.M.) for TNF-α immunoreactivities, measured by Western blotting and normalized to ponceau signals. Statistical analysis was performed using the one-way ANOVA followed by Tukey's multiple comparisons test, $n = 5$–10 independent samples; $^{***}p < 0.001$ (Y *vs* S); $^{\#\#}p < 0.01$ (S *vs* S + NAC). B) IL-6 release in the medium was evaluated by ELISA in Y, S, and S HUVECs following treatment with NAC after 24 and 48 h. The results are expressed in pg/mL (mean ± S.E.M.). Data were analysed by the one-way ANOVA followed by Tukey's multiple comparisons test, $n = 3$ independent samples; $^{****}p < 0.0001$ (Y *vs* S); $^{\#\#\#\#}p < 0.0001$ (S *vs* S + NAC). S + NAC 24 h = S cells after 24 h of NAC treatment; S + NAC 48 h = S cells after 48 h of NAC treatment.

et al., 2017; Sharpless and Sherr, 2015). The simultaneous activation of both pathways is a defining feature of "late senescence". While p21 often mediates the initial p53-dependent arrest, the subsequent rise in p16 is essential for making this arrest irreversible through epigenetic silencing of proliferative genes. The high expression of both markers in our old HUVECs confirms they have reached a stable state of terminal growth arrest.

A key novel insight of this study is that replicative aging in HUVECs is accompanied by a progressive and significant decline in the RNA-binding protein HuR expression. HuR is a master regulator of post-transcriptional gene expression, known for its ability to stabilize mRNAs involved in antioxidant defense stress responses and cell survival (Pascale and Govoni, 2012). Increasing evidence indicates that HuR expression and function are impaired during cellular aging (Varesi et al., 2023), and several studies have shown that HuR loss promotes senescence by destabilizing transcripts implicated in proliferative processes or encoding cytoprotective proteins and antioxidant enzymes (Varesi et al., 2023; Wang et al., 2001). Moreover, since HuR knockdown has been linked to the upregulation of SASP-related cytokines [IL-6, chemokine ligand 2 (Ccl-2), and vascular endothelial growth factor], the senescence markers p16 and p21, and the metalloprotease 2, as well as to an arrest of cellular proliferation (Varesi et al., 2023), its reduction in our model may likely contributes to the amplification of OS and inflammatory signaling, reinforcing the senescent phenotype and endothelial dysfunction. Taken together, these observations provide compelling evidence that late-passage HUVECs transition toward a state of consolidated senescence, driven by an imbalance between loss of protective factors (HuR) and accumulation of damage-response markers (ROS, p21, p16). Our data also support the concept that the loss of HuR is not merely a consequence of aging, but a driver of the senescent phenotype.

In light of the growing global elderly population, identifying effective therapeutic approaches to prevent and/or treat age-associated diseases has become a clinical priority. In this context, we focused on NAC, a multifaceted agent widely used to restore intracellular glutathione levels across various metabolic, pulmonary, and hepatic disorders (Elbini Dhouib et al., 2016). NAC operates primarily as a senomorphic by reducing OS, which helps suppress the inflammatory signals (SASP) generated by aging cells. Unlike potent senolytics (*e.g.*, dasatinib, navitoclax), which can induce severe systemic toxicities like thrombocytopenia or neutropenia, NAC, globally accessible and FDA-approved as an antioxidant/mucolytic and acetaminophen antidote, has an established, highly favourable safety profile with minimal side effects even at high chronic doses (Gurău et al., 2018; Tenório et al., 2021). Most other senotherapeutics are still restricted to clinical trials or lack standardized regulatory approval for aging (Kirkland and Tchkonia, 2020). With a view to using as senotherapeutics in prevention, we decided to use NAC instead of other molecules, such as quercetin, because NAC acts upstream to mitigate initial cellular damage and inflammation, while quercetin (senolytic agent) serves as a selective tool to actively remove already-aged cells. Quercetin, rather than merely quieting senescent cells, blocks survival pathways (such as PI3K/AKT), thereby forcing these cells to undergo apoptosis. This flavonoid is much more effective at clearing core markers of deep senescence (p16 and SA-β-galactosidase) (Abharzanjani et al., 2017; Luo et al., 2023), especially when combined with other compounds like dasatinib (Liu et al., 2026).

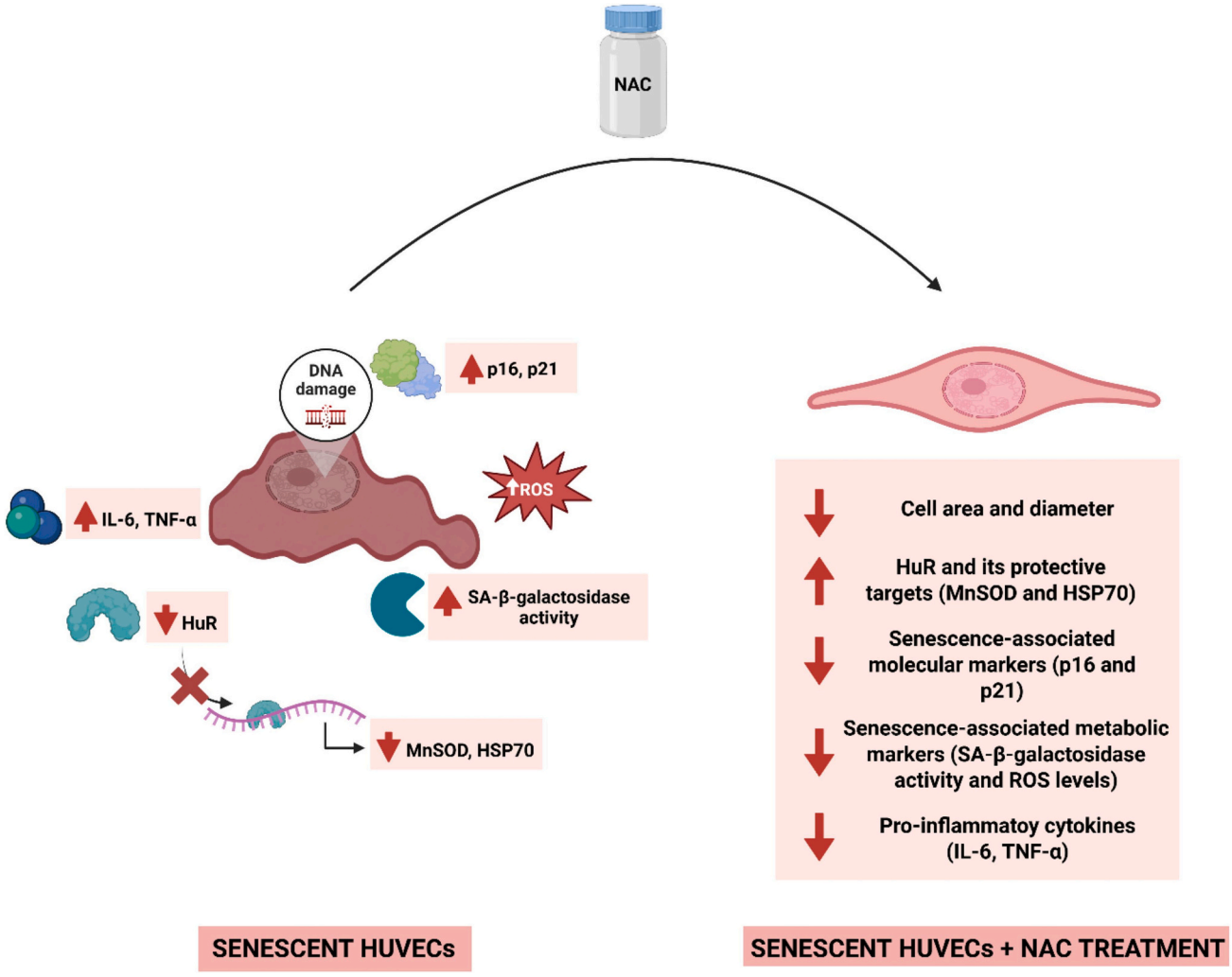

Fig. 7. Effect of *N*-acetylcysteine treatment on late-passage HUVECs. Late-passage HUVECs exhibit characteristic features of cellular senescence, including morphological alterations (increased cell area and diameter), elevated senescence-associated metabolic markers (SA-β-galactosidase activity and intracellular ROS), loss of proliferative capacity (upregulation of p21 and p16), increased pro-inflammatory cytokines (IL-6 and TNF-α) alongside reduced expression of HuR and its protective targets (MnSOD and HSP70). NAC treatment effectively counteracts these hallmarks by restoring HuR-dependent pathways, reducing senescence-associated molecular and metabolic markers, and suppressing the pro-inflammatory phenotype. (Created with Biorender.com; licence to the Department of Drug Sciences, University of Pavia).
Abbreviations: HSP70: heat shock proteins 70; HUVECs: human umbilical vein endothelial cells; IL-6: interleukin 6; MnSOD: manganese-dependent superoxide dismutase; NAC: *N*-acetylcysteine; ROS: reactive oxygen species; SA: senescence-associated; TNF-α: tumour necrosis factor α.

However, quercetin, while widely available as a supplement and showing great promise, has a less predictable absorption rate in the body and is still heavily undergoing human clinical trials to fully prove its efficacy as an anti-aging therapy (Liu et al., 2025).

Our initial assessment focused on whether NAC could affect the senescent phenotype morphologically. We observed a discernible trend toward a more organized cellular architecture and a reduction in both cell area and diameter in NAC-treated senescent HUVECs (Fig. 3), suggesting a shift toward a "young-like" profile. This structural trend likely reflects an underlying biochemical reprogramming, which we further investigated at the molecular level. Indeed, our findings reveal that NAC treatment markedly reduced intracellular ROS levels in senescent HUVECs, restoring them to values comparable to those of young cells. This outcome aligns with NAC's well-documented antioxidant properties, acting both as a direct ROS scavenger and as a precursor for glutathione synthesis (Pedre et al., 2021). In parallel, NAC reduced the expression of key senescence-associated markers. Notably, p21 levels significantly decreased after 24 h of treatment and reached baseline (young) levels by 48 h. This evidence supports the notion that p21 is highly sensitive to redox status; since ROS induce p21 expression and p21, in turn, amplifies ROS production, NAC effectively disrupts this pro-senescent positive feedback loop (Passos et al., 2010). In contrast, p16 showed only a modest, non-significant reduction. This observation is consistent with the evidence that p16 is less tied to ROS and linked to more stable epigenetic/transcriptional programs that are less responsive to acute antioxidant intervention (Overhoff et al., 2014). Similarly, the slower response of SA-β-galactosidase activity to NAC —which persisted even when experiments were extended to 72 h—suggests that certain structural and lysosomal features of the senescent phenotype are highly stable and require either prolonged intervention or distinct enzymatic clearance kinetics for full reversal. Therefore, this delayed response likely represents a genuine biological feature of deep senescence rather than a mere limitation of an insufficient treatment window.

A major insight of this study is the significant restoration of HuR expression in senescent HUVECs after NAC treatment. This observation supports the concept that OS negatively impacts HuR stability and function (Ferrigno et al., 2023; Mehta et al., 2016), suggesting that NAC preserves HuR expression and/or prevents its degradation, thereby

reinforcing post-transcriptional regulatory networks critical for cellular homeostasis. The regulatory interplay between NAC and HuR expression highlighted in our study warrants further mechanistic consideration. HuR expression and RNA-binding activity are highly sensitive to the intracellular redox environment. Excessive OS disrupts HuR function by promoting redox-dependent post-translational modifications and altering its interaction with target mRNAs. Under selected stress conditions, prolonged cellular stress may also reduce HuR protein stability through proteasome-dependent degradation (Abdelmohsen et al., 2009, 2007; Chu et al., 2012). At the post-translational level, high ROS levels have been shown to induce modifications that accelerate HuR protein degradation, such as targeted ubiquitination leading to proteasomal clearance (Srikantan and Gorospe, 2012) or the activation of specific caspases that cleave HuR. Crucially, our real-time PCR analysis demonstrates that NAC treatment also modulates HuR at the transcriptional level, significantly increasing its mRNA expression at 48 h. This implies that the impact of redox homeostasis on HuR is comprehensive, extending from protein stability to transcript lifetime. Therefore, it can be speculated that, by efficiently scavenging intracellular ROS and replenishing GSH pools, NAC counteracts the oxidative triggers that drive both HuR protein degradation and transcriptional repression. Alternatively, given that HuR is well established to regulate its own expression through a positive feedback loop by binding to the 3′-untranslated region of its own mRNA (Grammatikakis et al., 2017), NAC might primarily rescue the HuR protein content from oxidative degradation; the restored HuR protein, in turn, would actively promote the stabilization and accumulation of its own transcript. Consistent with HuR recovery, NAC also upregulated its targets MnSOD and HSP70. In line with our results, several studies have highlighted reduced MnSOD expression in senescent cells (Treiber et al., 2011; Velarde et al., 2012), which contributes to mitochondrial dysfunction and excessive ROS production (Gavriilidis et al., 2013). Furthermore, MnSOD depletion is also associated with increased senescence markers, including p16, p21, and SA-β-galactosidase activity (Li et al., 2018). Similarly, HSP70 levels decline with aging (Murshid et al., 2013), leading to impaired proteostasis and increased sensitivity to cellular stress (Ruano, 2021). The restoration of MnSOD and HSP70 observed in our work suggests that NAC enhances endothelial stress resistance through HuR-dependent post-transcriptional mechanisms.

Lastly, senescent HUVECs exhibited a pronounced pro-inflammatory phenotype (SASP), characterized by elevated TNF-α and IL-6. Notably, these cytokines are key mediators of chronic, low-grade inflammation and are known to accelerate and reinforce cellular senescence *via* positive feedback loops (Freund et al., 2010; Kandhaya-Pillai et al., 2017). NAC significantly reduced this inflammatory profile: while IL-6 decreased rapidly, TNF-α showed a delayed but robust reduction. These data confirm NAC's anti-inflammatory effects, likely mediated *via* its antioxidant properties or the modulation of redox-sensitive signaling pathways, such as NF-κB (Santus et al., 2024; Tenório et al., 2021).

5. Conclusion

Our work further consolidated the evidence that late-passage HUVECs reach a state of established senescence, characterized by morphological shifts, metabolic changes (increased SA-β-galactosidase activity and intracellular ROS levels), loss of proliferative capacity (upregulation of the cyclin-dependent kinase inhibitors p21 and p16), and increase in pro-inflammatory cytokines (IL-6 and TNF-α) (Fig. 7). Importantly, the present study provides the first evidence for a decline in the HuR-protective axis in senescent HUVECs. Moreover, our results highlight the multifaceted potential of NAC to counteract some of these hallmarks (morphology shift, intracellular ROS levels, and p21 protein expression) by activating HuR-dependent protective pathways at both transcriptional and protein levels, and attenuating inflammation. Collectively, these findings identify HuR as a novel player in the promotion of a senescent phenotype and position NAC as a promising candidate for mitigating aging and its associated pathologies.

CRediT authorship contribution statement

Lucrezia Irene Maria Campagnoli: Writing – original draft, Visualization, Software, Methodology, Investigation, Formal analysis, Data curation. **Nicoletta Marchesi:** Visualization, Methodology, Formal analysis, Data curation, Conceptualization. **Annalisa Barbieri:** Visualization, Formal analysis, Data curation. **Nicoletta Galeotti:** Visualization, Supervision, Formal analysis, Data curation. **Alessia Pascale:** Writing – review & editing, Writing – original draft, Visualization, Supervision, Formal analysis, Data curation, Conceptualization.

Funding

The authors have nothing to report.

Declaration of competing interest

The authors declare no conflicts of interest.

Acknowledgments

We acknowledge the financial contribution of FRG2025 from the University of Pavia to L.I.M.C. The authors wish to thank Dr. Amanda Oldani of “Centro Grandi Strumenti” of the University of Pavia for her support and technical assistance provided to the confocal and widefield microscopy.

Appendix A. Supplementary data

Supplementary data to this article can be found online at https://doi.org/10.1016/j.exger.2026.113257.

Data availability

Data will be made available on request.

References

Abdelmohsen, K., Pullmann, R., Lal, A., Kim, H.H., Galban, S., Yang, X., Blethrow, J.D., Walker, M., Shubert, J., Gillespie, D.A., Furneaux, H., Gorospe, M., 2007. Phosphorylation of HuR by Chk2 regulates SIRT1 expression. Mol. Cell 25, 543–557. https://doi.org/10.1016/j.molcel.2007.01.011.

Abdelmohsen, K., Srikantan, S., Yang, X., Lal, A., Kim, H.H., Kuwano, Y., Galban, S., Becker, K.G., Kamara, D., De Cabo, R., Gorospe, M., 2009. Ubiquitin-mediated proteolysis of HuR by heat shock. EMBO J. 28, 1271–1282. https://doi.org/10.1038/emboj.2009.67.

Abharzanjani, F., Afshar, M., Hemmati, M., Moossavi, M., 2017. Short-term high dose of quercetin and resveratrol alters aging markers in human kidney cells. Int. J. Prev. Med. 8. https://doi.org/10.4103/ijpvm.IJPVM_139_17.

Al Bitar, S., Gali-Muhtasib, H., 2019. The role of the cyclin dependent kinase inhibitor p21cip1/waf1 in targeting cancer: molecular mechanisms and novel therapeutics. Cancers 11, 1475. https://doi.org/10.3390/cancers11101475.

Amadio, M., Scapagnini, G., Laforenza, U., Intrieri, M., Romeo, L., Govoni, S., Pascale, A., 2008. Post-transcriptional regulation of HSP70 expression following oxidative stress in SH-SY5Y cells: the potential involvement of the RNA-binding protein HuR. CPD 14, 2651–2658. https://doi.org/10.2174/138161208786264052.

Amaya-Montoya, M., Pérez-Londoño, A., Guatibonza-García, V., Vargas-Villanueva, A., Mendivil, C.O., 2020. Cellular senescence as a therapeutic target for age-related diseases: a review. Adv. Ther. 37, 1407–1424. https://doi.org/10.1007/s12325-020-01287-0.

Bloom, S.I., Islam, M.T., Lesniewski, L.A., Donato, A.J., 2023. Mechanisms and consequences of endothelial cell senescence. Nat. Rev. Cardiol. 20, 38–51. https://doi.org/10.1038/s41569-022-00739-0.

Campagnoli, L.I.M., Ahmad, L., Marchesi, N., Greco, G., Boschi, F., Masi, F., Mallucci, G., Bergamaschi, R., Colombo, E., Pascale, A., 2024. Disclosing the novel protective mechanisms of Ocrelizumab in multiple sclerosis: the role of PKC Beta and its downstream targets. Int. J. Mol. Sci. 25, 8923. https://doi.org/10.3390/ijms25168923.

Childs, B.G., Gluscevic, M., Baker, D.J., Laberge, R.-M., Marquess, D., Dananberg, J., Van Deursen, J.M., 2017. Senescent cells: an emerging target for diseases of ageing. Nat. Rev. Drug Discov. 16, 718–735. https://doi.org/10.1038/nrd.2017.116.

Chu, P.-C., Chuang, H.-C., Kulp, S.K., Chen, C.-S., 2012. The mRNA-stabilizing factor HuR protein is targeted by β-TrCP protein for degradation in response to glycolysis

inhibition. J. Biol. Chem. 287, 43639–43650. https://doi.org/10.1074/jbc.M112.393678.
Coluzzi, E., Leone, S., Sgura, A., 2019. Oxidative stress induces telomere dysfunction and senescence by replication fork arrest. Cells 8, 19. https://doi.org/10.3390/cells8010019.
Cong, Y., Li, X., Hong, H., 2025. Current strategies for senescence treatment: focused on theranostic performance of nanomaterials. J. Control. Release 382, 113710. https://doi.org/10.1016/j.jconrel.2025.113710.
Elbini Dhouib, I., Jallouli, M., Annabi, A., Gharbi, N., Elfazaa, S., Lasram, M.M., 2016. A minireview on N -acetylcysteine: an old drug with new approaches. Life Sci. 151, 359–363. https://doi.org/10.1016/j.lfs.2016.03.003.
Fahmideh, F., Marchesi, N., Campagnoli, L.I.M., Landini, L., Caramella, C., Barbieri, A., Govoni, S., Pascale, A., 2022. Effect of troxerutin in counteracting hyperglycemia-induced VEGF upregulation in endothelial cells: a new option to target early stages of diabetic retinopathy? Front. Pharmacol. 13, 951833. https://doi.org/10.3389/fphar.2022.951833.
Ferrigno, A., Campagnoli, L.I.M., Barbieri, A., Marchesi, N., Pascale, A., Croce, A.C., Vairetti, M., Di Pasqua, L.G., 2023. MCD diet modulates HuR and oxidative stress-related HuR targets in rats. Int. J. Mol. Sci. 24, 9808. https://doi.org/10.3390/ijms24129808.
Franco, A.C., Martini, H., Victorelli, S., Lagnado, A.B., Wyles, S.P., Rowsey, J.L., Pirius, N., Woo, S., Costa, D.G., Chaib, S., Tullius, S.G., Tchkonia, T., Kirkland, J.L., Khosla, S., Jurk, D., Cavadas, C., Passos, J.F., 2025. Senescent cell transplantation into the skin induces age-related peripheral dysfunction and cognitive decline. Aging Cell 24, e14340. https://doi.org/10.1111/acel.14340.
Freund, A., Orjalo, A.V., Desprez, P.-Y., Campisi, J., 2010. Inflammatory networks during cellular senescence: causes and consequences. Trends Mol. Med. 16, 238–246. https://doi.org/10.1016/j.molmed.2010.03.003.
Gavriilidis, C., Miwa, S., Von Zglinicki, T., Taylor, R.W., Young, D.A., 2013. Mitochondrial dysfunction in osteoarthritis is associated with down-regulation of superoxide dismutase 2. Arthritis Rheum. 65, 378–387. https://doi.org/10.1002/art.37782.
Gorgoulis, V., Adams, P.D., Alimonti, A., Bennett, D.C., Bischof, O., Bishop, C., Campisi, J., Collado, M., Evangelou, K., Ferbeyre, G., Gil, J., Hara, E., Krizhanovsky, V., Jurk, D., Maier, A.B., Narita, M., Niedernhofer, L., Passos, J.F., Robbins, P.D., Schmitt, C.A., Sedivy, J., Vougas, K., Von Zglinicki, T., Zhou, D., Serrano, M., Demaria, M., 2019. Cellular senescence: defining a path forward. Cell 179, 813–827. https://doi.org/10.1016/j.cell.2019.10.005.
Grammatikakis, I., Abdelmohsen, K., Gorospe, M., 2017. Posttranslational control of HuR function. WIREs RNA 8. https://doi.org/10.1002/wrna.1372.
Grosse, L., Wagner, N., Emelyanov, A., Molina, C., Lacas-Gervais, S., Wagner, K.-D., Bulavin, D.V., 2020. Defined p16High senescent cell types are indispensable for mouse healthspan. Cell Metab. 32, 87–99.e6. https://doi.org/10.1016/j.cmet.2020.05.002.
Gurău, F., Baldoni, S., Prattichizzo, F., Espinosa, E., Amenta, F., Procopio, A.D., Albertini, M.C., Bonafè, M., Olivieri, F., 2018. Anti-senescence compounds: a potential nutraceutical approach to healthy aging. Ageing Res. Rev. 46, 14–31. https://doi.org/10.1016/j.arr.2018.05.001.
Hernandez-Segura, A., Nehme, J., Demaria, M., 2018. Hallmarks of cellular senescence. Trends Cell Biol. 28, 436–453. https://doi.org/10.1016/j.tcb.2018.02.001.
Herranz, N., Gil, J., 2018. Mechanisms and functions of cellular senescence. J. Clin. Invest. 128, 1238–1246. https://doi.org/10.1172/JCI95148.
Jomova, K., Raptova, R., Alomar, S.Y., Alwasel, S.H., Nepovimova, E., Kuca, K., Valko, M., 2023. Reactive oxygen species, toxicity, oxidative stress, and antioxidants: chronic diseases and aging. Arch. Toxicol. 97, 2499–2574. https://doi.org/10.1007/s00204-023-03562-9.
Kandhaya-Pillai, R., Miro-Mur, F., Alijotas-Reig, J., Tchkonia, T., Kirkland, J.L., Schwartz, S., 2017. TNFα-senescence initiates a STAT-dependent positive feedback loop, leading to a sustained interferon signature, DNA damage, and cytokine secretion. Aging 9, 2411–2435. https://doi.org/10.18632/aging.101328.
Kaur, J., Farr, J.N., 2020. Cellular senescence in age-related disorders. Transl. Res. 226, 96–104. https://doi.org/10.1016/j.trsl.2020.06.007.
Khosla, S., Farr, J.N., Tchkonia, T., Kirkland, J.L., 2020. The role of cellular senescence in ageing and endocrine disease. Nat. Rev. Endocrinol. 16, 263–275. https://doi.org/10.1038/s41574-020-0335-y.
Kirkland, J.L., Tchkonia, T., 2020. Senolytic drugs: from discovery to translation. J. Intern. Med. 288, 518–536. https://doi.org/10.1111/joim.13141.
Lee, J.H., Jung, M., Hong, J., Kim, M.K., Chung, I.K., 2018. Loss of RNA-binding protein HuR facilitates cellular senescence through posttranscriptional regulation of TIN2 mRNA. Nucleic Acids Res. 46, 4271–4285. https://doi.org/10.1093/nar/gky223.
Li, Z., Liu, T., Ma, J., Guo, Q., Ma, L., Lv, Q., Jiang, Y., Wei, C., Zhang, J., 2018. TGF-β induces corneal endothelial senescence via increase of mitochondrial reactive oxygen species in chronic corneal allograft failure. Aging 10, 3474–3485. https://doi.org/10.18632/aging.101659.
Liu, L., Barber, E., Kellow, N.J., Williamson, G., 2025. Improving quercetin bioavailability: a systematic review and meta-analysis of human intervention studies. Food Chem. 477, 143630. https://doi.org/10.1016/j.foodchem.2025.143630.
Liu, J., Ren, X., Wang, H., Yang, D., Yan, Y., Xu, Y., 2026. Dasatinib and quercetin mitigate radiation-induced lung injury by eliminating senescent cells in a rat model. Front. Pharmacol. 17, 1748788. https://doi.org/10.3389/fphar.2026.1748788.
Luo, G., Xiang, L., Xiao, L., 2023. Quercetin alleviates atherosclerosis by suppressing oxidized LDL-induced senescence in plaque macrophage via inhibiting the p38MAPK/p16 pathway. J. Nutr. Biochem. 116, 109314. https://doi.org/10.1016/j.jnutbio.2023.109314.
Mallucci, G., Marchesi, N., Campagnoli, L.I.M., Boschi, F., Fahmideh, F., Fusco, S., Tavazzi, E., Govoni, S., Bergamaschi, R., Pascale, A., 2022. Evidence for novel cell defense mechanisms sustained by dimethyl fumarate in multiple sclerosis patients: the HuR/SOD2 cascade. Mult. Scler. Relat. Disord. 68, 104197. https://doi.org/10.1016/j.msard.2022.104197.
McHugh, D., Gil, J., 2018. Senescence and aging: causes, consequences, and therapeutic avenues. J. Cell Biol. 217, 65–77. https://doi.org/10.1083/jcb.201708092.
Mehta, M., Basalingappa, K., Griffith, J.N., Andrade, D., Babu, A., Amreddy, N., Muralidharan, R., Gorospe, M., Herman, T., Ding, W.-Q., Ramesh, R., Munshi, A., 2016. HuR silencing elicits oxidative stress and DNA damage and sensitizes human triple-negative breast cancer cells to radiotherapy. Oncotarget 7, 64820–64835. https://doi.org/10.18632/oncotarget.11706.
Mijit, M., Caracciolo, V., Melillo, A., Amicarelli, F., Giordano, A., 2020. Role of p53 in the regulation of cellular senescence. Biomolecules 10, 420. https://doi.org/10.3390/biom10030420.
Murshid, A., Eguchi, T., Calderwood, S.K., 2013. Stress proteins in aging and life span. Int. J. Hyperth. 29, 442–447. https://doi.org/10.3109/02656736.2013.798873.
Ngo, V., Duennwald, M.L., 2022. Nrf2 and oxidative stress: a general overview of mechanisms and implications in human disease. Antioxidants (Basel, Switzerland) 11, 2345. https://doi.org/10.3390/antiox11122345.
Overhoff, M.G., Garbe, J.C., Koh, J., Stampfer, M.R., Beach, D.H., Bishop, C.L., 2014. Cellular senescence mediated by p16INK4A-coupled miRNA pathways. Nucleic Acids Res. 42, 1606–1618. https://doi.org/10.1093/nar/gkt1096.
Pascale, A., Govoni, S., 2012. The complex world of post-transcriptional mechanisms: is their deregulation a common link for diseases? Focus on ELAV-like RNA-binding proteins. Cell. Mol. Life Sci. 69, 501–517. https://doi.org/10.1007/s00018-011-0810-7.
Passos, J.F., Nelson, G., Wang, C., Richter, T., Simillion, C., Proctor, C.J., Miwa, S., Olijslagers, S., Hallinan, J., Wipat, A., Saretzki, G., Rudolph, K.L., Kirkwood, T.B.L., Von Zglinicki, T., 2010. Feedback between p21 and reactive oxygen production is necessary for cell senescence. Mol. Syst. Biol. 6, 347. https://doi.org/10.1038/msb.2010.5.
Pedre, B., Barayeu, U., Ezeriņa, D., Dick, T.P., 2021. The mechanism of action of N-acetylcysteine (NAC): the emerging role of H2S and sulfane sulfur species. Pharmacol. Ther. 228, 107916. https://doi.org/10.1016/j.pharmthera.2021.107916.
Rayess, H., Wang, M.B., Srivatsan, E.S., 2012. Cellular senescence and tumor suppressor gene p16. Int. J. Cancer 130, 1715–1725. https://doi.org/10.1002/ijc.27316.
Ruano, D., 2021. Proteostasis dysfunction in aged mammalian cells. The stressful role of inflammation. Front. Mol. Biosci. 8, 658742. https://doi.org/10.3389/fmolb.2021.658742.
Santus, P., Signorello, J.C., Danzo, F., Lazzaroni, G., Saad, M., Radovanovic, D., 2024. Anti-inflammatory and anti-oxidant properties of N-acetylcysteine: a fresh perspective. J. Clin. Med. 13, 4127. https://doi.org/10.3390/jcm13144127.
Sharpless, N.E., Sherr, C.J., 2015. Forging a signature of in vivo senescence. Nat. Rev. Cancer 15, 397–408. https://doi.org/10.1038/nrc3960.
Srikantan, S., Gorospe, M., 2012. HuR function in disease. Front. Biosci. (Landmark Ed) 17, 189–205. https://doi.org/10.2741/3921.
Tenório, M.C.D.S., Graciliano, N.G., Moura, F.A., Oliveira, A.C.M.D., Goulart, M.O.F., 2021. N-acetylcysteine (NAC): impacts on human health. Antioxidants 10, 967. https://doi.org/10.3390/antiox10060967.
Treiber, N., Maity, P., Singh, K., Kohn, M., Keist, A.F., Ferchiu, F., Sante, L., Frese, S., Bloch, W., Kreppel, F., Kochanek, S., Sindrilaru, A., Iben, S., Högel, J., Ohnmacht, M., Claes, L.E., Ignatius, A., Chung, J.H., Lee, M.J., Kamenisch, Y., Berneburg, M., Nikolaus, T., Braunstein, K., Sperfeld, A., Ludolph, A.C., Briviba, K., Wlaschek, M., Scharffetter-Kochanek, K., 2011. Accelerated aging phenotype in mice with conditional deficiency for mitochondrial superoxide dismutase in the connective tissue. Aging Cell 10, 239–254. https://doi.org/10.1111/j.1474-9726.2010.00658.x.
Varesi, A., Chirumbolo, S., Campagnoli, L.I.M., Pierella, E., Piccini, G.B., Carrara, A., Ricevuti, G., Scassellati, C., Bonvicini, C., Pascale, A., 2022. The role of antioxidants in the interplay between oxidative stress and senescence. Antioxidants (Basel, Switzerland) 11, 1224. https://doi.org/10.3390/antiox11071224.
Varesi, A., Campagnoli, L.I.M., Barbieri, A., Rossi, L., Ricevuti, G., Esposito, C., Chirumbolo, S., Marchesi, N., Pascale, A., 2023. RNA binding proteins in senescence: a potential common linker for age-related diseases? Ageing Res. Rev. 88, 101958. https://doi.org/10.1016/j.arr.2023.101958.
Velarde, M.C., Flynn, J.M., Day, N.U., Melov, S., Campisi, J., 2012. Mitochondrial oxidative stress caused by Sod2 deficiency promotes cellular senescence and aging phenotypes in the skin. Aging 4, 3–12. https://doi.org/10.18632/aging.100423.
Wang, W., Yang, X., Cristofalo, V.J., Holbrook, N.J., Gorospe, M., 2001. Loss of HuR is linked to reduced expression of proliferative genes during replicative senescence. Mol. Cell. Biol. 21, 5889–5898. https://doi.org/10.1128/MCB.21.17.5889-5898.2001.
Yi, S., Lin, K., Jiang, T., Shao, W., Huang, C., Jiang, B., Li, Q., Lin, D., 2020. NMR-based metabonomic analysis of HUVEC cells during replicative senescence. Aging 12, 3626–3646. https://doi.org/10.18632/aging.102834.